PRELIMINARY ANALYSIS OF THE EARTHQUAKE (MW 8.1) AND TSUNAMI OF APRIL 1, 2007, IN THE SOLOMON ISLANDS, SOUTHWESTERN PACIFIC OCEAN

Michael A. Fisher, Eric L. Geist, Ray Sliter, Florence L. Wong, Carol Reiss, and Dennis M. Mann

U.S. Geological Survey,

345 Middlefield Rd., MS 999, Menlo Park, California, USA

ABSTRACT

On April 1, 2007, a destructive earthquake (Mw 8.1) and tsunami struck the central Solomon Islands arc in the southwestern Pacific Ocean. The earthquake had a thrust-fault focal mechanism and occurred at shallow depth (between 15 km and 25 km) beneath the island arc. The combined effects of the earthquake and tsunami caused dozens of fatalities and thousands remain without shelter. We present a preliminary analysis of the Mw-8.1 earthquake and resulting tsunami. Multichannel seismic-reflection data collected during 1984 show the geologic structure of the arc's frontal prism within the earthquake's rupture zone. Modeling tsunami-wave propagation indicates that some of the islands are so close to the earthquake epicenter that they were hard hit by tsunami waves as soon as 5 min. after shaking began, allowing people scant time to react.

1. INTRODUCTION

The M-8.1 earthquake in the Solomon Islands that occurred at 20:40 on April 1, 2007 (UTC), struck along a complicated plate boundary in the southwestern Pacific Ocean (Figure 1). Earthquake shaking and a tsunami caused as many as 52 fatalities and left thousands homeless (Reliefweb, 2007a). These figures remain unconfirmed because the affected area is impoverished and remote from government resources. Clearly, however, this earthquake's aftermath includes considerable human suffering.

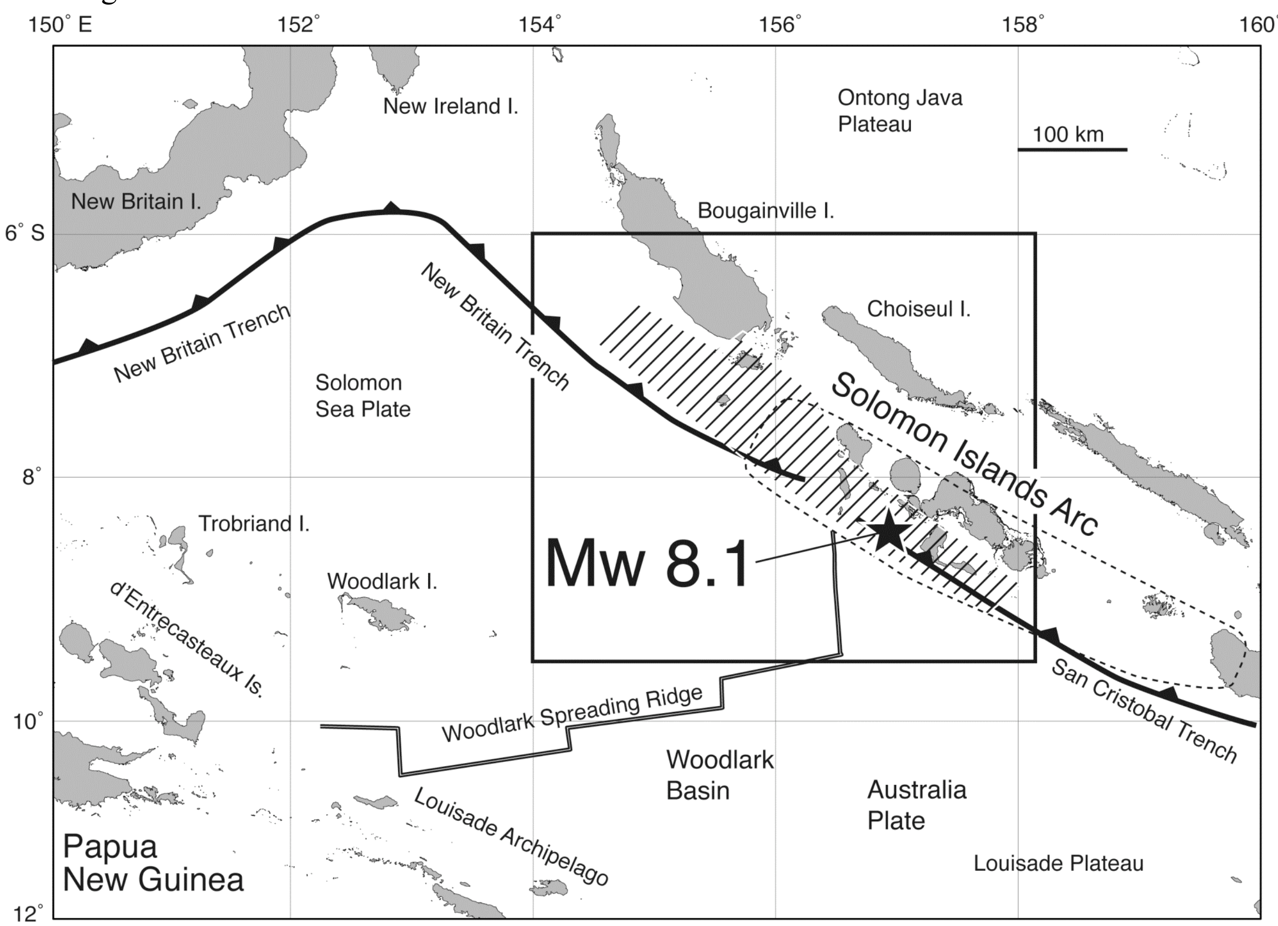

Figure 1. Index map of the part of the southwest Pacific Ocean that includes the Solomon Islands arc and the epicenter of the 2007 Mw-8.1 subduction-zone earthquake. The crosshatched area shows the rupture zone of the 2007 earthquake. The dotted outline shows the part of the island arc that has been characterized by a reduced level of historical seismicity (Cooper and Taylor, 1987). The box shows the area included in Figure 2a. Plate-convergence rates and directions are from Mann et al. (1998).

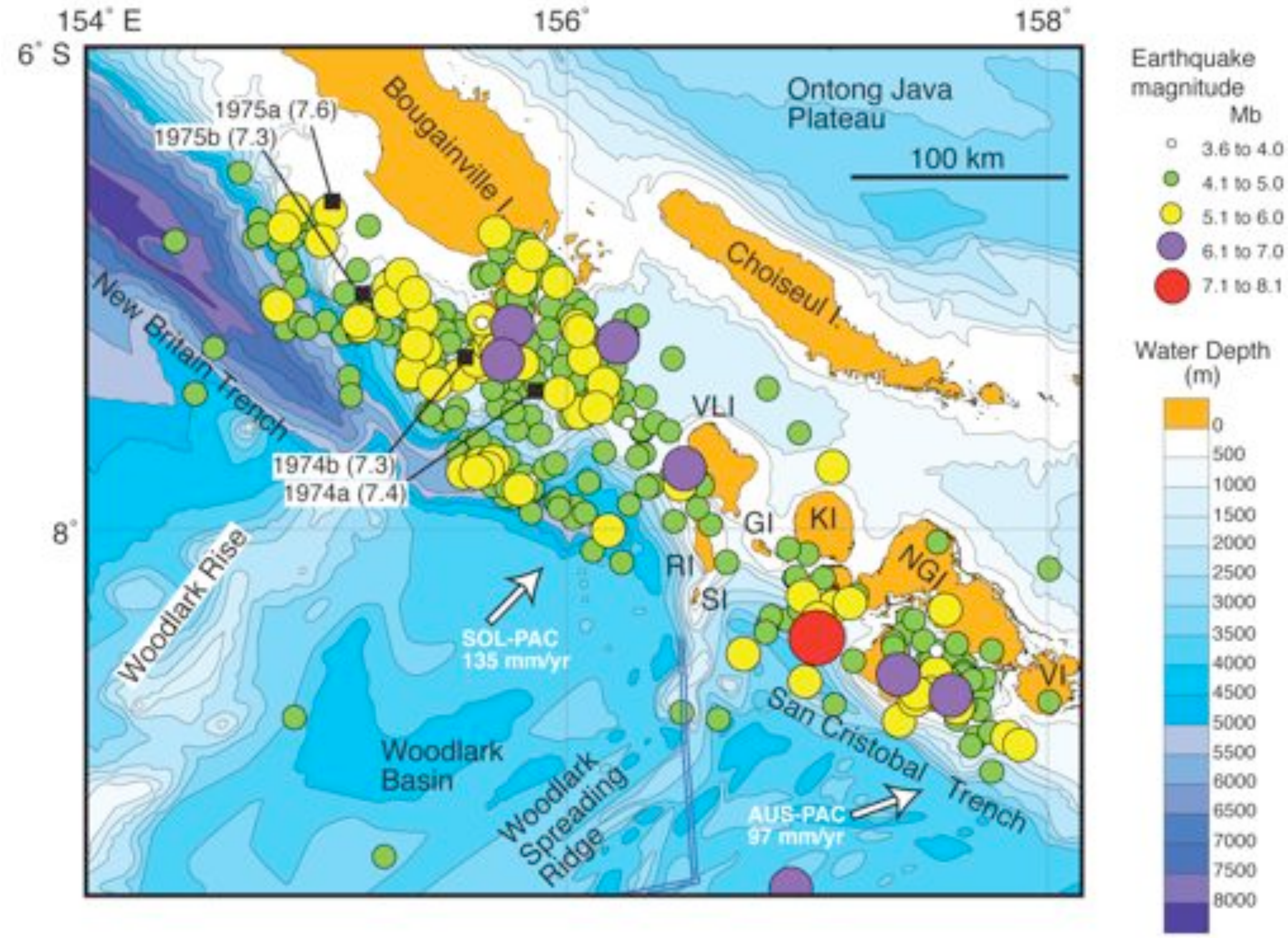

Figure 2a. Location of main shock (red circle) and aftershocks of the 2007 Mw-8.1 earthquake. Plate-convergence rates and directions are from Mann et al. (1998). Black squares and numbers like "1975a (7.6) " give year, sequence and magnitude of doublet earthquakes that occurred in the rupture zone of the 2007 earthquake. Figure area given in Figure 1. GI: Ghizo Island. KI: Kolombangara Island. NBT: New Britain Trench. NGI: New Georgia Island. RI: Ranongga Island. SCT: San Cristobol Trench. SI: Simbo Island. VI: Vangunu Island: VLI: Vela Lavella Island.

The Solomon Islands arc lies along the southwestern boundary of the Pacific plate, and the Mw-8.1 earthquake was a subduction-zone thrust event. Several aspects of geography and geology make this earthquake and tsunami unique. First, although young oceanic crust is being subducted eastward at the New Britain Trench, the down going plate bends sharply downward and dips steeply (30˚ to 45˚) into the mantle, and the earthquake's epicenter is located almost beneath the trench axis (Figure 2a). Second, in the past 30 years, numerous earthquake doublets have struck this island arc (e.g. Lay and Kanamori, 1980), and the rupture zone of the 2007 earthquake includes the locations of two doublets, having magnitudes of about M 7 (Figure 2a). To date (9/1/2007), however, the 2007 event has produced aftershocks as large as Mb 6.6, but no second M-8 earthquake and tsunami have occurred.

Third, where the earthquake struck, complex bathymetric and tectonic elements, including an active spreading ridge and transform fault, are being subducted. The effect of ridge subduction on seismogenesis is evident from the fact that earthquake slip began southeast of where the spreading ridge enters the subduction zone; slip was reduced directly over the ridge; and northwest of the ridge, slip resumed with increased amplitude.

2. GEOLOGIC SETTING OF THE EPICENTRAL REGION

Since the middle Miocene, the Ontong Java Plateau (Figure 1) has been colliding with the trench along the east side of the Solomon Islands arc (Kroenke, 1972; Mann and Taira, 2004; Phinney et al., 1999). This collision caused eastward subduction of oceanic crust to commence along the west side of the arc, forming an exemplar of subduction-polarity reversal (e.g. Karig and Mammerickx, 1972). Earthquake hypocenters indicate that oceanic crust on both the east and the west sides of the island arc is being subducted (e.g. Cooper and Taylor, 1985, 1987; Shinohara et al., 2003; Yoneshima et al., 2005).

The 2007 Mw-8.1 earthquake occurred along the west side of the arc, where the New Britain and San Cristobal Trenches mark the northeastward subduction of the oceanic plates on the west. This crust includes the Solomon Sea plate to the north and the Australia plate to the south across the Woodlark spreading ridge (Figure 1). Plate convergence between the Solomon Sea and Pacific plates, is rapid, amounting to about 100 mm/yr (Bird, 2003; Tregoning et al., 1998).

The Woodlark spreading ridge extends discontinuously eastward across the Woodlark Basin to where the ridge is being underthrust at the New Britain Trench, along the west side of the Solomon Islands arc (Goodliffe, et al., 1999; Martinez, et al., 1999; Taylor, 1999; Taylor and Exon, 1987; Weissel et al., 1982)(Figure 1). The spreading ridge figures prominently in this study because the ridge enters the trench only about 50 km northwest of the epicenter for the 2007 earthquake (Figure 2b). North of the Woodlark spreading ridge, the New Britain Trench deepens northwestward, from about 5 km near the ridge to as deep as 8 km west of Bougainville Island (Figure 1 and 2a). Across the spreading ridge to the southeast, the San Cristobal trench is not well expressed bathymetrically, at depths of 4 km to 5 km.

The Woodlark spreading ridge became active about 6 Ma ago (Taylor et al., 1999), and modeling geodetic data indicates that the current half-spreading rate across the ridge increases progressively eastward toward the New Britain Trench, where the half-rate may be as much as 40 mm/yr (Tregoning et al., 1998).

This spreading ridge is segmented by several transform faults (e.g. Martinez et al., 1999; Taylor et al., 1999). In particular, near the New Britain Trench the Simbo transform fault extends northward from a spreading-ridge segment (Figure 2b) to obliquely underthrust the arc's frontal prism. Swath-bathymetric data indicate that the transform fault widens northeastward, which has been interpreted as evidence for crustal spreading along this transform fault since about 80 ka (Martinez et al., 1999).

Ghizo Ridge, possibly an extinct segment of the spreading-ridge, is surmounted by seamounts and extends southeastward along the axis of the San Cristobal Trench (Figure 2b). The epicenter of the 2007 earthquake is located just northeast of Ghizo Ridge and within a re-entrant in the forearc slope.

The Simbo bathymetric ridge, distinct from the transform fault, extends northward across the forearc slope and supports Simbo and Ranongga Islands (Figure 2b). These islands are near the trench axis and were among the areas hardest hit by the 2007 tsunami. Simbo Ridge and its surmounting islands apparently formed owing to subduction of the Woodlark spreading ridge. In this area, spreading-ridge subduction mainly controls the location and intensity of near-trench volcanism (e.g. Johnson et al., 1987; Taylor and Exon, 1987). Near the epicenter of the 2007 earthquake, volcanism is restricted in occurrence to the area of New Georgia Island, east of where the spreading ridge is being subducted. Near-trench volcanoes that formed Simbo Island actually lie west of the projected location of the trench axis, and other volcanoes lie within just 30 km of this axis.

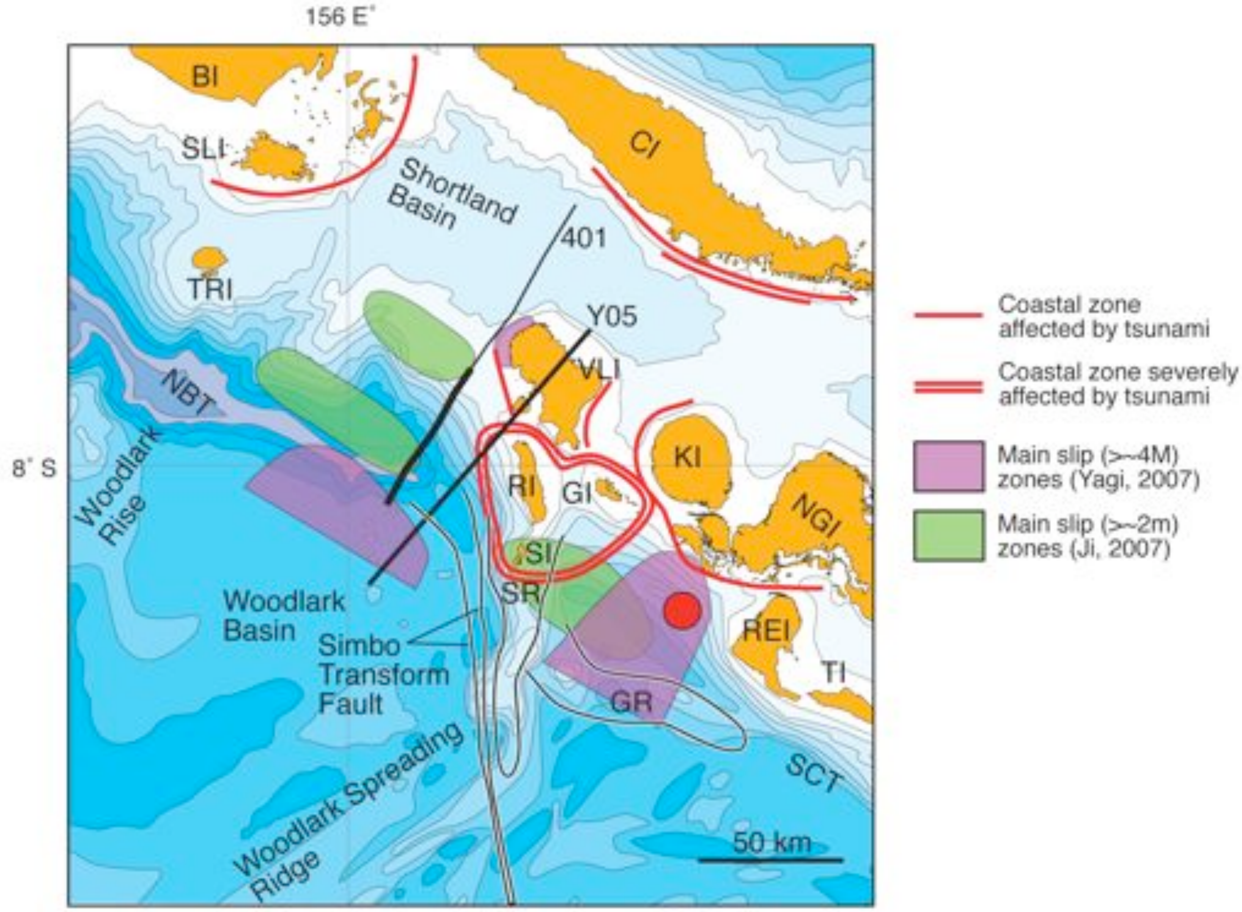

Figure 2b. The areas most severely affected by the tsunami include the near-trench islands of Simbo, Ghizo and Ranongga and the southwest coast of Choiseul Island. Red circle shows the epicenter of the 2007 Mw-8.1 earthquake. The main fault-slip zones during the 2007 earthquake are separated by the subducted Simbo transform fault. Figure area given in Figure 2a. Location of MCS section 401 in Figures 3a and 3b is shown by the heavy part of the black line labeled “401”. The line of section showing locally recorded hypocenters used in Figures 3b and 3c is shown by the black line labeled “Y05”. Abbreviations as in Figure 2a except for: BI: Bougainville Island. CI: Choiseul Island. GR: Ghizo ridge. REI: Rendova Island. TI: Tetepare Island. SLI: Shortland Island. SR: Simbo ridge. TRI: Treasury Island.

Another geologic consequence of ridge subduction is vertical tectonic motion of local forearc areas. For example, Mann et al. (1998) and Taylor et al. (2005) described a high spatial variation in uplift rates, near New Georgia Island, that the authors attribute to subduction of the irregular lower-plate bathymetry. The 2007 epicenter is located within a re-entrant in the lower arc slope (Figure 2b). Similar forearc re-entrants are scars caused by the subduction of high standing bathymetric features (e.g. Fisher et al., 1991; Geist et al., 1993). How tectonic processes associated with ridge subduction affected earthquake and tsunami generation are topics for further research.

3. THE 2007 EARTHQUAKE (MW 8.1)

Cooper and Taylor (1987) noted that epicenters of shallow (<70 km) and intermediate (70 km to 130 km) focal-depth earthquakes are uncommon in the central part of the island arc, as outlined in Figure 1. This central area coincides with the locus of subduction of the Woodlark spreading center (Cooper and Taylor, 1987). The epicenter for the 2007 earthquake occurred within the central zone of reduced seismicity (Figure 1), thus filling at least the northwestern half of the seismic gap.

Global CMT Catalog data (CMT, 2007) indicate that the main shock was located at 7.96˚ S and 156.40˚ E at a depth of 23 km, and the nodal plane showing thrust-fault motion strikes 331˚ and dips northeast at 38˚. Two other estimates of the attitude of the nodal plane yielded broadly similar values. According to Yagi (2007), the strike is 300˚ and the dip 19˚, whereas Ji (2007) estimated the strike to be 305˚ and dip 25˚. Fault rupture propagated northwestward from the epicenter at a mean velocity of 1.95 km/s (Yagi, 2007). The rupture zone of the 2007 earthquake extended at least 250 km along the Solomon Islands arc. Within the two-month period following the main shock, as many as 10 aftershocks with Mb between 6 and 7 had occurred.

The Solomon Islands subduction zone is noted for producing earthquake doublets--two earthquakes having similar magnitude that occur closely in space and time (Kagan and Jackson, 1999; Lay and Kanamori, 1980; Schwartz, 1999; Xu and Schwartz, 1993). The mechanism causing earthquake doublets remains controversial, although stress triggering of the second earthquake by the first one in the doublet is likely to be a significant factor. Kagan and Jackson (1999) discuss the period between doublet earthquakes.

The largest historic doublet to strike this island arc occurred 12 days apart during 1971 and involved a pair of M-8.0 and -8.1 earthquakes north of Bougainville Island (Schwartz et al., 1989). After the 2007 Mw-8.1 earthquake, despite deep concerns among disaster workers, a follow-on earthquake and tsunami have not struck.

Most earthquake doublets in the Solomon Islands have occurred north of the 2007 epicenter, in the vicinity of Bougainville Island and along the northwest-striking part of the New Britain Trench. Two doublets during 1974 and 1975 were located within the northwestern part of the 2007 rupture zone (Xu and Schwartz, 1993) (Figure 2a). The four events making up these doublets ranged in Mw from 7.3 to 7.6, and their focal mechanisms were compatible with underthrusting and subduction of the western oceanic plate. Xu and Schwartz (1993) proposed that the 1974 and 1975 doublets originated owing to the roughness of the oceanic plate that is being subducted because the Woodlark Rise enters the New Britain Trench west of the epicenters.

Subduction of high standing bathymetric features has demonstrably affected fault slip during the 2007 earthquake. According to two finite fault models (Ji, 2007; Yagi, 2007), fault rupture bridged across the subducted part of the active Woodlark spreading ridge (Figure 2b). The finite fault models differ in detail, but they agree to the extent that they show two main slip zones and a third small zone near Vella Lavella Island. However, the slip zones by Yagi (2007) are shifted southwest from, and indicate a slip magnitude nearly twice as great as, the slip zones and magnitude presented by Ji (2007). Both models indicate that one of the two main slip zones surrounded the earthquake's epicenter and that the zones are separated by an area of slip deficit located where the Woodlark spreading ridge and the Simbo transform fault are being subducted. In both models, the second or northwestern main slip zone does not extend northwest of where the Woodlark Rise enters the trench (Figure 2b), hence this bathymetric feature may have formed a barrier to earthquake rupture.

4. SEISMIC-REFLECTION SECTION THROUGH THE EARTHQUAKE RUPTURE ZONE

During 1984, the U.S. Geological Survey collected multichannel seismic-reflection (MCS) data in the Solomon Islands arc (e.g. Bruns et al., 1989b). Seismic line 401 (Figs. 3a and 3b) from this survey crosses the rupture zone of the 2007 earthquake (Figure 2b). Another version of this seismic section is shown and interpreted in Bruns et al. (1989a). For this report, we reprocessed the seismic section, migrating these data after stack and using sonobuoy-refraction velocities obtained over the lower slope and Shortland basin (Cooper et al., 1986a,b, 1989) to produce a depth section without vertical exaggeration (Figure 3b).

MCS section 401 reveals flat reflections from the interplate decollement that can be followed for more than 40 km east of the trench (Figure 3a). These events separate discontinuous and weak reflections from within the superjacent frontal prism of the island arc from more continuous reflections from lower-plate rocks. The time and the depth-converted MCS sections (Figs. 3a and 3b) reveal rocks under the decollement that dip consistently southeastward and terminate against the abrupt seafloor rise that borders the New Britain Trench on the southeast. This rise is located along the Simbo transform fault. Swath bathymetry shows that this transform fault strikes north, nearly perpendicular to the seismic section, and the fault widens toward the New Britain Trench (Martinez et al., 1998) (Figure 2b). Lower-plate rocks that dip southeast and abut the transform fault appear to fill a half graben (Figs. 3a and 3b). This half graben may have resulted from the crustal spreading along this transform fault that occurred since about 80 ka (Martinez et al., 1999), but the graben fill may be too thick (~2 km) to have resulted solely from such a short period of extension. Alternatively, the velocity used in the depth conversion is wrong and exaggerates the thickness.

To estimate the location of the interplate boundary northwest of where reflections from the decollement end on MCS section 401, we plotted locally recorded hypocenters, instead of teleseismically located ones, on the depth section (Figure 3b) and on a regional cross section (Figure 3c). The local hypocenters were determined from data obtained during a deployment of ocean-bottom seismometers in 1998 (Yoneshima et al. 2005). Yoneshima et al. (2005) used these hypocenters to show that the seismic front underlies the upper slope, consistently below the 1000 m isobath, and that the down going plate dips ~30° northeast through the zone of highest seismic activity, which is deeper than about 20 km. The water bottom multiple on MCS section 401 becomes a wide band of persistent

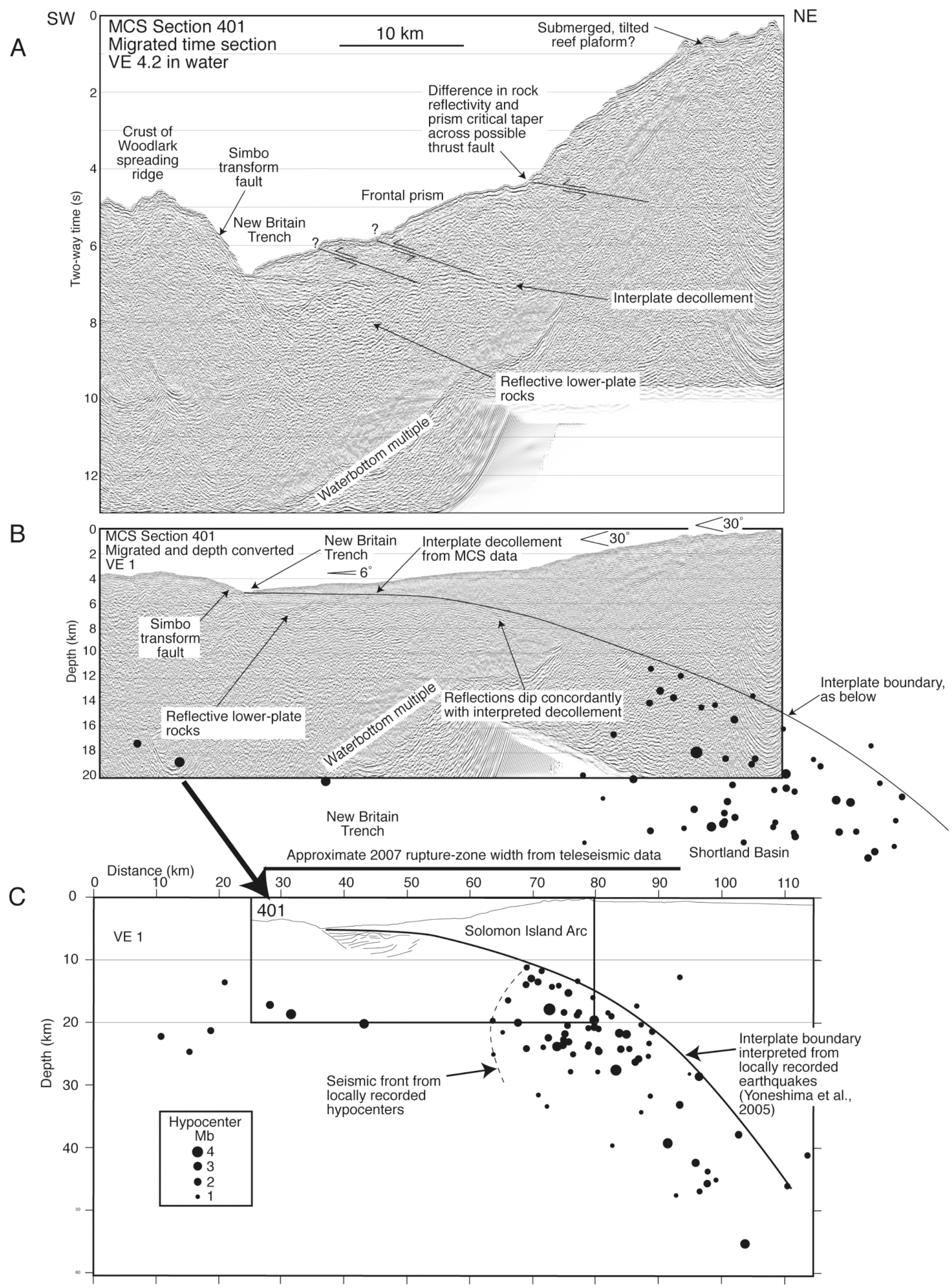

Figure 3a. Migrated time section of U.S. Geological Survey seismic line. Section location shown in Figure 2b by the black line annotated "401".

noise when migrated (Figure 3a), and it prevents us from making a direct connection between the decollement indicated by reflections and the interplate boundary indicated by hypocenters.

Three seafloor discontinuities over the frontal prism may signify active thrust faults (Figs. 3a and 3b). The two discontinuities closer to the trench occur where reflections from within the prism are poor, so the faults are speculative. However, reflections from near the shallowest seafloor discontinuity yield better evidence for a thrust fault in that rocks at shallow depth on the fault's upslope side are more reflective and thicker than are rocks on the down slope side. Recent research interest has focused on the role in tsunamigenesis played by splay thrust faults that deform a frontal prism, especially in studies conducted off the Nankai Trough (e.g. Bangs et al., 2004; Kondo et al., 2005; Park et al., 2000, 2002). Concerning the 2007 earthquake in the Solomon Islands, we currently lack sufficient information to determine whether thrust faults interpreted from MCS section 401 (Figs. 3a and 3b) were active during the earthquake, but their potential role is a topic for future research.

The shallowest interpreted thrust fault coincides with an abrupt change in the critical taper of the wedge (Figs. 3a and 3b). Over the lowermost slope, the wedge critical taper is 6˚ whereas at the shallowest fault, the taper increases to 30˚, and the taper maintains this value eastward to beyond the shelf break (Figure 3b). At other subduction zones, variations in the critical taper of the frontal prism provide clues to how and where major earthquakes might nucleate along an interplate decollement (Wang and Hu, 2006; Kimura et al., 2007). Furthermore, Kimura et al. (2007) discuss the Nankai accretionary prism and link variations in critical wedge taper to specific structural styles within the wedge and to mechanical properties along the decollement. In the analysis by Wang and Hu (2006) the break in slope between a forearc basin and the outboard accretionary prism coincides with the outward-directed change in frictional properties along the decollement from velocity-weakening to velocity-strengthening. Hence, in this analysis the slope break is proposed to overlie the updip end of the seismogenic zone.

These findings are difficult to apply straightforwardly to the case of the Solomon Islands arc near MCS line 401 because the nearby subduction of the Woodlark spreading ridge, with its irregular bathymetry and probable high heat flow, injects a strongly three-dimensional aspect into the analysis. However, the half graben associated with the Simbo transform fault thins northeastward and appears to die out altogether below the increase in critical taper (Figure 3a). Thus the critical-taper increase from 6˚ to 30˚ may coincide with a change in frictional properties across the decollement: presumably northwest of where the graben ends, lower-plate rocks just under the decollement are igneous oceanic crust instead of sedimentary graben fill. This lithologic change might form the updip limit of the seismogenic zone.

The seismic section shows what may be pinnacle reefs under shallow water near the shelf break (Figure 3a). If they are reefs, then their flat upper surfaces indicate previous sea levels and the present depth of the pinnacles indicates submergence and southeastward tilting of the shelf edge. This may be evidence for subduction erosion of the upper plate by high standing bathymetric features thrust beneath the island arc.

5. THE TSUNAMI

According to news reports, the areas most severely affected by tsunami inundation include the near-trench islands of Simbo, Ranongga, and especially Ghizo (e.g. Unosat, 2007) as well as the southwest coast of Choiseul Island, which lies east of the Shortland Basin (Figure 2b). Reportedly, the tsunami waves were between two and ten meters high and swept inland for almost half a kilometer (Alertnet, 2007). Thirty-three of the 52 tsunami victims died on the most severely impacted island of Ghizo, and 21 victims on this island were children (Alertnet, 2007; Reliefweb, 2007b). The government of the Solomon Islands estimated that 30,000 people were affected by the earthquake and tsunami. After the tsunami, many villages lacked suitable housing. Homes were swept away because of the primitive construction techniques traditionally employed on the islands. Most houses have roofs thatched with Sago palm leaves and supported by wooden poles. Many people remain in makeshift hilltop camps, too frightened to return to coastal villages. Mental health issues among the affected populace are of greater concern than is rebuilding, according to a team from the Asian Development Bank, which is working with the government on an emergency assistance project (Disasternews, 2007). The humanitarian disaster attending the earthquake and tsunami led to a convention of many government agencies to determine what lessons were learned that would aid recovery in case of a future disaster (Reliefweb, 2007c).

The 2007 Solomon Islands seism does not appear to have been a "tsunami earthquake," defined as one that produces a tsunami of far greater intensity than would be expected from the considering the earthquake's magnitude alone (Kanamori, 1972; Kanamori and Kikuchi, 1993; Polet and Kanamori, 2000). The teleseismically determined location for the epicenter of the 2007 earthquake is close to the axis of the San Cristobal trench, and a near-trench epicenter characterizes tsunami earthquakes.

However, observations concerning the 2007 earthquake do not accord with the other characteristics of tsunami earthquakes listed in Polet and Kanamori (2000). Perhaps most significant is the observed rupture velocity of 1.95 km/s (Yagi, 2007), which is higher than the low (as low as 1 km/s) rupture velocity typical of tsunami earthquakes (e.g., Ihmlé, 1996; López and Okal, 2006).

A more likely cause for the near-trench epicenter is the warm slab, including an active spreading center, that is being subducted. A warm slab is thought to shift the seismogenic zone up dip along the plate interface and to widen this zone, relative to the cold-slab case (Kirby, 2000; Peacock and Hyndman, 1999; Peacock et al., 1999).

An exceptional tsunami could be caused by an earthquake rupturing inside a sedimentary wedge made up of weak material, which conceptually could lead to enhanced seafloor motion (Fukao, 1979; Okal, 1988). However, MCS data from the Solomon Island arc (Figure 3b) indicate that at least in the northwest part of the rupture area of the 2007 earthquake, the frontal prism is narrow, measured horizontally and perpendicular to the trench, and thin.

Although the 2007 tsunami had dire consequences for the Solomon Islands, the transoceanic tsunami generated by this earthquake had only low amplitude (NGDC, 2007; NOAA, 2007). For example, along the northeast coast of Australia, about 1600 km away from the epicenter, the wave amplitude was about 0.1 m.

To create a preliminary numerical simulation of the April 2007 tsunami, we started with the fault mechanism determined by the Global CMT Project (CMT 2007). The length of the fault that ruptured was determined from the distribution of aftershocks and from seismic inversions (Ji, 2007; Yagi, 2007).The tsunami-source and -propagation model is based on the method in an earlier study (Geist and Parsons, 2005) that investigated tsunamis from the November 2000 New Ireland earthquake sequence. Animations showing the propagation of the 2007 Solomon Islands tsunami are available on the internet (http://soundwaves.usgs.gov/2007/04/).

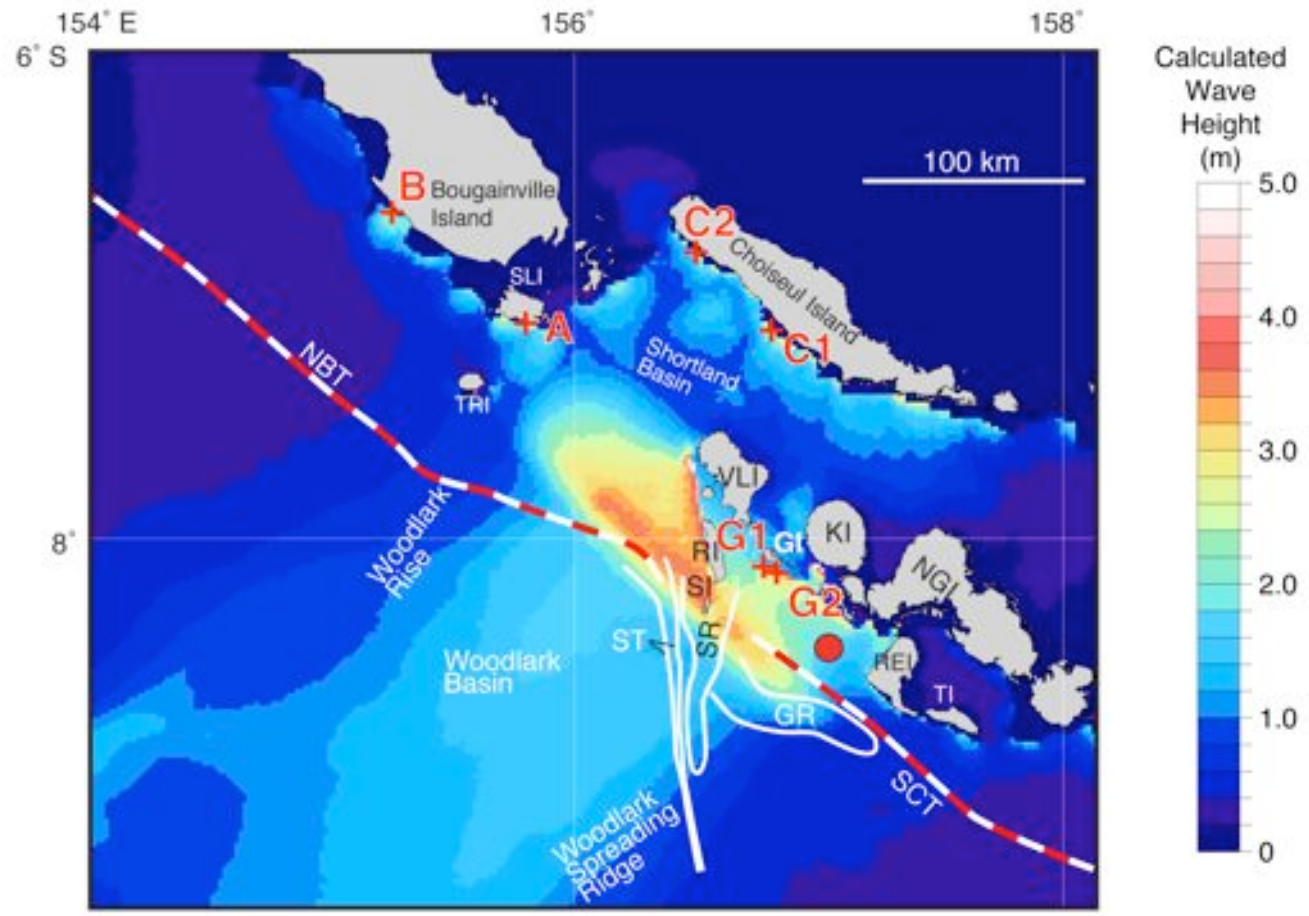

Figure 4. Numerical propagation model of the 2007 tsunami, based on the method in Geist and Parsons (2005). The geographic area depicted here is the same as in Figure 2a. Colors show the distribution of maximum calculated tsunami amplitude that occurred during the first 73 min. of tsunami propagation. Red circle locates the epicenter of the Mw-8.1 earthquake. Dashed red and white lines show trench axes. Red crosses show the locations of the marigrams in Figure 5. Red letters near these crosses refer to specific marigrams. B: Bougainville. C1: Choiseul1. C2: Choiseul2. G1:Ghizo1. G2: Ghizo2. Other abbreviations are as in Figures 2a and 2b.

Coarse-grid propagation modeling is useful for determining the open-ocean beaming pattern for the tsunami. This modeling indicates that the highest offshore amplitudes occurred near the islands of Simbo, Ghizo and Ranungga (Figure 4a), which accords with news reports. It is important to note, however, that this modeling does not account for propagation near shore, where water is less than 100 m deep. Modeling shallow-water propagation requires high-resolution bathymetry (Titov and Synolakis, 1998). We await field measurements of tsunami inundation to better constrain the tsunami modeling. Also, tsunami modeling can be further refined using the specific slip distribution for this earthquake derived from seismic-waveform analysis (Ji, 2007; Yagi, 2007).

Offshore synthetic marigrams derived from our tsunami modeling indicate that the first tsunami wave arrived at hard-hit Ghizo Island within just 5 min. after the earthquake, and contrary to common expectation, the ocean apparently did not withdraw prior to the tsunami's arrival (Figure 5A). The brief period between the onset of the earthquake and the tsunami's arrival denied people time to realize the imminent danger and react accordingly. In contrast, at islands like Choiseul that are farther away from the trench significant wave heights arrived as much as 20 min. after the earthquake (Figure 5B). Local areas along the coast of Bougainville Island that face the New Britain Trench may have experienced some inundation (Figure 5C).

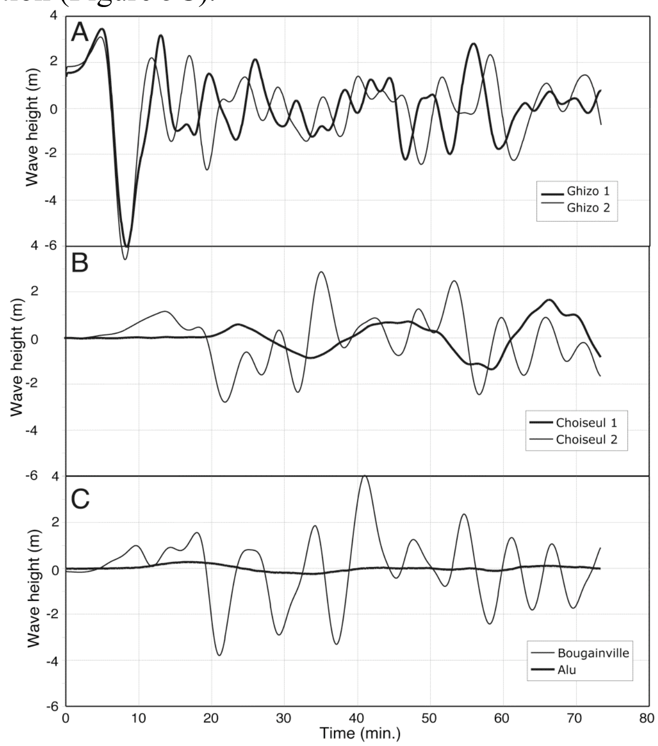

Figure 5A. Synthetic offshore marigrams from the numerical tsunami model showing the calculated wave height for at locations near Ghizo Island, which suffered the worst inundation, for 73 min. after the earthquake. Marigram locations are shown in Figure 4. Water depths at Ghizo1 and Ghizo2 are 142 m and 104 m, respectively.

Figure 5B. Synthetic offshore marigrams near the west coast of Choiseul Island. Marigram locations are shown in Figure 4. Water depths at Choiseul1 and Choiseul2 are 114 m and 114 m, respectively.

Figure 5C. Synthetic offshore marigrams near the west and southwest coasts of Bougainville Island. Marigram locations are shown in Figure 4. Water depths at Bougainville and Alu are 155m and 134 m, respectively.

6. CONCLUSION

The Mw-8.1 earthquake and tsunami that struck the Solomon Islands on April 1, 2007, had substantial long-term impact on local population centers. This earthquake-driven tsunami revealed particular challenges for government agencies in trying to warn local population centers, because only a short time passed between the onset of shaking and arrival of tsunami waves.

The geologic complexity of the plate boundary where the 2007 earthquake struck provides fertile ground for future research. Reprocessing MCS data from other parts of the earthquake's rupture zone will promote better understanding about the origin of this and other tsunamis that originate in subduction zones. Other research topics include the influence of ridge subduction on seismogenesis and the role of splay thrust faults deforming the frontal prism in the generation of tsunamis.

REFERENCES

Alertnet (2007). http://www.alertnet.org/thenews/fromthefield/219478/117984356860.htm

CMT (2007). http://neic.usgs.gov/neis/eq_depot/2007/eq_070401_aqbk/neic_aqbk_hrv.html

Bangs, N. L. B., Shipley, T. H., Gulick, S., Moore, G. F., Kuromoto, S., and Nakamura, Y. (2004). Evolution of the Nankai Trough decollement from the trench into the seismogenic zone: Inferences from three-dimensional seismic reflection imaging: Geology, v. 32, p. 273-276.

Bird, P. (2003). An updated digital model of plate boundaries: G3, v. 4, doi:10.1029/2001GC000252, p. 52 p.

Bruns, T. R., Vedder, J. G., and Cooper, A. K. (1989a). Geology of the Shortland basin region, central Solomons Trough, Solomon Islands--review and new findings, in Vedder, J. G., and Bruns, T. R., eds., Geology and offshore resources of Pacific island arcs--Solomon Islands and Bougainville, Papua New Guinea regions, v. 12: Houston, Texas, Circum-Pacific Council for Energy and Minearal Resources, p. 125-144.

Bruns, T. R., Vedder, J. G., Hart, P. E., and Mann, D. M. (1989b). Multichannel seismic-reflection profiles across the Solomon Islands arc: Guadalcanal-Malaita, Vella Lavella-Choiseul and Bougainville-Buka regions, in Vedder, J. G., and Bruns, T. R., eds., Geology and offshore resources of Pacific island arcs--Solomon Islands and Bougainville, Papua New Guinea regions, v. 12: Houston, Texas, Circum-Pacific Council for Energy and Minearal Resources, p. 323-328.

Cooper, A. K., Bruns, T. R., and Wood, R. A. (1986). Shallow crustal structure of the Solomon Islands intra-arc basins from sonobuoy seismic studies, in Vedder, J. G., Pound, K. S., and Boundy, S. Q., eds., Geology and offshore resources of Pacific island arcs--central and western Solomon Islands, v. 4: Houston, Texas, Circum-Pacific Council for Energy and Minearal Resources, p. 135-156.

Cooper, A. K., Cochrane, G. R., and Bruns, T. R. (1989). Velocity-structure of the upper crust beneath the Solomon Islands-Bougainville island arc, in Vedder, J. G., and Bruns, T. R., eds., Geology and offshore resources of Pacific island arcs--Solomon Islands and Bougainville, Papua New Guinea regions, v. 12: Houston, Texas, Circum-Pacific Council for Energy and Minearal Resources, p. 23-46.

Cooper, A. K., Marlow, M. S., and Bruns, T. R. (1986). Deep structure of the central and southern Solomon Islnads region: Implications for tectonic origin, in Vedder, J. G., Pound, K. S., and Boundy, S. Q., eds., Geology and offshore resources of Pacific island arcs--central and western Solomon Islands, v. 4: Houston, Texas, Circum-Pacific Council for Energy and Minearal Resources, p. 157-175.

Cooper, P. A., and Taylor, B. (1985). Polarity reversal in the Solomon Islands arc: Nature, v. 314, p. 428-430.

Cooper, P. A., and Taylor, B. (1987). A geophysical survey of the Woodlark-Solomons region, in Taylor, B., and Exon, N. F., eds., Marine Geology Geophysics, and Geochemistry of the Woodlark Basin-Solomon Islands, Earth Sci. Ser., v 7: Houston, Texas, Circum-Pac. Counc. Energy Mineral Resour, p. 67-88.

Disasternews, 2007, http://www.disasternews.net/news/article.php?articleid=3213

Fisher, M. A., Collot, J. Y., and Geist, E. L. (1991). Structure of the collision zone between Bougainville guyot and the accretionary wedge of the New Hebrides Island arc, southwest Pacific: Tectonics, v. 10, p. 887-903.

Fukao, Y. (1979). Tsunami earthquake and subduction processes near deep sea trenches: J. Geophys. Res, v. 84, p. 2303-2314.

Geist, E. L., Fisher, M. A., and Scholl, D. W. (1993). Large-scale deformation associated with ridge subduction: Geophys. J. Inter., v. 115, p. 344-366.

Geist, E. L., and Parsons, T. (2005). Triggering of tsunamigenic aftershocks from large strike-slip earthquake: Analysis of the November 2000 New Ireland earthquake sequence: G3, doi:10.1029/2005GC000935, v. 6, p. 1-18.

Goodliffe, A. M., Taylor, B., and Martinez, F. (1999). Data report: Marine geophysical surveys of the Woodlark Basin region, in Taylor, B., Huchon, P., and Klaus, A., eds., Proc. ODP, Init. Repts., 180, 1-134 [CD-ROM]: College Station, TX 77845-9547, U.S.A., Ocean Drilling Program, Texas A&M University.

Ihmlé, P.F. (1996). Frequency-dependent relocation of the 1992 Nicaragua slow earthquake: an empirical Green's function approach. Geophys. J. Internat., v. 127, p. 75-85.

Ji, C. (2007). Rupture process of the 2007 April 1, Magnitude 8.1, Solomon Islands Earthquake: http://earthquake.usgs.gov/eqcenter/eqinthenews/2007/us2007aqbk/finite_fault.php.

Johnson, R. W., Jaques, A. L., Langmuir, C. H., Perfit, M. R., Staudigel, H., Dunkley, P. N., Chappell, B. W., Taylor, S. R., and Baekisapa, M. (1987). Ridge subduction and forearc volcanism: petrology and geochemistry of rocks dredged from the western Solomon island arc and Woodlark Basin (no copy), in Taylor, B., and Exon, N. F., eds., Marine Geology Geophysics, and Geochemistry of the Woodlark Basin-Solomon Islands, Earth Sci. Ser., v 7: Houston, Texas, Circum-Pac. Counc. Energy Mineral Resour, p. 155-226.

Kagan, Y. Y., and Jackson, D. D. (1999). Worldwide doublets of large shallow earthquakes: J. Geophys. Res, v. 89, p. 1147-1155.

Kanamori, H. (1972). Mechanism of tsunami earthquakes: Physics Earth Planetary Interiors, v. 6, p. 346-359.

Kanamori, H. and Kikuchi, M. (1993). The 1992 Nicaragua earthquake: a slow earthquake associated with subducted sediments. Nature, 361: 714-716.

Karig, D. E., and Mammerickx, J. (1972). Tectonic framework of the New Hebrides Island arc: Marine Geology, v. 12, p. 187-205.

Kimura, G., Kitamura, Y., Hashimoto, Y., Yamaguchi, A., Shibata, T., Ujie, K., and Okamoto, S. (2007). Transition of accretionary wedge structures around the up-dip limit of the seismogenic subduction zone: Earth and Planetary Science Letters, v. 255, p. 471-484.

Kirby, S. H. (2000). Taking the temperature of slabs: Nature, v. 403, p. 31-34.

Kondo, H., Kimura, G., Masago, H., Ohmori-Ikehara, K., Kitamura, Y., Ikesawa, E., Sakaguchi, A., Yamaguchi, A., and Okamoto, S. (2005). Deformation and fluid flow of a major out-of-sequence thrust located at seismogenic depth in an accretionary complex: Nobeoka thrust in the Shimanto belt, Kyushu, Japan: Tectonics, v. 24, doi 10.1029/2004TC001655, 16 p.

Kroenke, L. W. (1972). Geology of the Ontong Java Plateau: Hawaii Institute of Geophysics report HIG-72-5, 119 p.

Lay, T., and Kanamori, H. (1980). Earthquake doublets in the Solomon Islands: Physics Earth Planetary Interiors, v. 21, p. 283-304.

López, A.M. and Okal, E.A. (2006). A seismological reassessment of the source of the 1946 Aleutian "tsunami" earthquake. Geophysical Journal International, 165: 835-849.

Mann, P., Taylor, F. W., Lagoe, M. B., Quarles, A., and Burr, G. (1998). Accelerating late Quaternary uplift of the New Georgia Island group (Solomon Island arc) in response to subduction of the recently active Woodlark spreading center and Coleman seamount: Tectonophysics, v. 295, p. 259-306.

Mann, P., and Taira, A. (2004). Global tectonic significance of the Solomon Islands and Ontong Java Plateau convergent zone: Tectonophysics, v. 389, p. 191-220.

Martinez, F., Taylor, B., and Goodliffe, A. M. (1999). Contrasting styles of seafloor spreading in the Woodlark Basin; indications of rift-induced secondary mantle convection: J. Geophys. Res., v. 104, p. 12,909-12,926.

NGDC (2007). http://www.ngdc.noaa.gov/nndc/struts/results?EQ_0=3037&t=101650&s=9&d=100,91,95,93&nd=display

NOAA (2007). http://www.prh.noaa.gov/ptwc/messages/pacific/2007/pacific.2007.04.02.040500_obs.txt

Okal, E. A. (1988). Seismic parameters controlling far-field tsunami amplitudes: a review: Natural Hazards, v. 1, p. 67-96.

Park, J. O., Tsuru, T., Kodaira, S., Nakanishi, A., Mirua, S., Kaneda, Y., and Kono, Y. (2000). Out-of-sequence thrust faults developed in the coseismic slip zone of the 1946 Nankai earthquake (Mw=8.2) off Shikoku, southwest Japan: Geophysical Research Letters, v. 27, p. 1033-1036.

Park, J. O., Tsuru, T., Kodaira, S., Cummins, P. R., and Kaneda, Y. (2002). Splay fault branching along the Nankai subduction zone: Science, v. 297, p. 1157-1160.

Peacock, S., and Hyndman, R. D. (1999). Hydrous minerals in the mantle wedge and the maximum depth of subduction thrust earthquakes: Geophys. Res. Lett., v. 26, p. 2517-2520.

Peacock, S., Wang, K., and McMahon, A. M. (1999). Seismic consequences of warm versus cool subduction metamorphism: Science, v. 286, p. 937-939.

Phinney, E. J., Mann, W. P., Coffin, M. P., and Shipley, T. H. (1999). Sequence stratigraphy, structure, and tectonic history of the southwestern Ontong Java Plateau adjacent to the North Solomon trench and Solomon Islands arc: J. Geophys. Res, v. 104, p. 20,449-20,466.

Polet, J., and Kanamori, H. (2000). Shallow subduction zone earthquakes and their tsunamigenic potential: Geophys. J. Inter., v. 142, p. 684-702.

Radio New Zealand (2007).
http://www.radionz.co.nz/news/latest/200706041508/6000_homes_destroyed_in_solomons_tsunami

Reliefweb (2007a). http://www.reliefweb.int/rw/RWB.NSF/db900SID/TBRL73EMT6?OpenDocument

Reliefweb (2007b). http://www.reliefweb.int/rw/RWB.NSF/db900SID/EKOI73G7KZ?OpenDocument

Reliefweb (2007c). http://www.reliefweb.int/rw/RWB.NSF/db900SID/LSGZ74CBTA?OpenDocument

Schwartz, S. Y., Lay, T., and Ruff, L. J. (1989). Source process of the great 1971 Solomon Islands doublet: Physics Earth Planetary Interiors, v. 56, p. 294-310.

Schwartz, S. Y. (1999). Noncharacteristic behavior and complex recurrence of large subduction zone earthquakes: J. Geophys. Res, v. 104, p. 23, 111-23,125.

Shinohara, M., Suyehiro, K., and Murayama, T. (2003). Microearthquake seismicity in relation to double convergence around the Solomon Islands arc by ocean-bottom seismometer observation: Geophys. J. Internat., v. 153, p. 691-698.

Taylor, B. (1999). Background and regional setting, in Taylor, B., Huchon, P., Klaus, A., and al., e., eds., Proc. ODP, Init. Repts., 180, 1-134 [CD-ROM]. Available from: Ocean Drilling Program, : College Station, TX 77845-9547, U.S.A., Texas A&M University.

Taylor, B., and Exon, N. F. (1987). An investigation of ridge subduction in the Woodlark-Solomons region: introduction and overview, in Taylor, B., and Exon, N. F., eds., Marine Geology Geophysics, and Geochemistry of the Woodlark Basin-Solomon Islands, Earth Sci. Ser., v 7: Houston, Texas, Circum-Pac. Counc. Energy Mineral Resources, p. 1-24.

Taylor, B., Goodlife, A. M., and Martinez, F. (1999). How continents break up: Insights from Papua New Guinea: J. Geophys. Res, v. 104, p. 7497-7512.

Taylor, F. W., Mann, P., Bevis, M. G., Edwards, R. L., Cheng, H., Cutler, K. B., Gray, S. C., Burr, G. S., Beck, J. W., Phillips, D. A., Cabioch, G., and Recy, J. (2005). Rapid forearc uplift and subsidence caused by impinging bathymetric features: Examples from the New Hebrides and Solomon arcs: Tectonics, v. 24, doi:10.1029/2004TC001650, p. 23 p.

Titov, V.V. and Synolakis, C.E. (1998). Numerical modeling of tidal wave runup: J. Waterway, Port, Coastal, and Ocean Engineering, 124: 157-171.

Tregoning, P., Lambeck, K., Stolz, A., Morgan, P., McClusky, S. C., van der Beek, P., McQueen, H., Jackson, R. J., Little, R. P., Laing, A., and Murphy, B. (1998). Estimation of current plate motions in Papua New Guinea from Global Positioning System observations: J. Geophys. Res, v. 103, p. 12,181-12,203.

Unosat (2007). http://unosat.web.cern.ch/unosat/asp/prod_free.asp?id=81

Wang, K., and Hu, Y. (2006). Accretionary prisms in subduction earthquake cycles: the theory of dynamic Coulomb wedge: J. Geophys. Res, v. 111, doi:10.1029/2005JB004094, 16 pp.

Weissel, J. K., Taylor, B., and Karner, G. D. (1982). The opening of the Woodlark basin, subduction of the Woodlark spreading system, and the evolution of northern Melanesia since mid-Pliocene time: Tectonophysics, v. 87, p. 253-277.

Xu, Z., and Schwartz, S. Y. (1993). Large earthquake doublets and fault plane heterogeniety in the northern Solomon Islands subduction zone: PAGEOPH, v. 140, p. 365-391.

Yagi, Y. (2007). http://www.geo.tsukuba.ac.jp/press_HP/yagi/EQ/20070401/

Yoneshima, S., Mochizuki, K., Araki, E., Hino, R., Shinohara, M., and Suyehiro, K. (2005). Subduction of the Woodlark Basin at the New Britain Trench, Solomon Islands region: Tectonophysics, v. 397, p. 225-239.